

# A Novel Segmentation Approach to Diagnose the Brain Tumor

Remya.R<sup>1</sup>, Parimala Geetha.K<sup>2</sup>

<sup>1</sup>Arunachala College of Engineering for Women, India, e-mail: [remiamernath@gmail.com](mailto:remiamernath@gmail.com))

<sup>2</sup>Nalla Malla Reddy Engineering College, India.

---

## Abstract

For an abnormal growth of tissues in the human body, usually Doctor's may examine their status through MR (Magnetic Resonance) scan images. For analyzing the position, a novel segmentation approach is proposed precisely here. Initially it performs morphological filtering operation by Top-Hat filtering to enhance the quality of an image. The morphological filtered output then undergoes segmentation to extract the brain tumor region alone. Such segmentation operation is done through our novel approach. It improves the segmentation performance level. Then comparison on the segmented output with the ground truth images is made with five performance measures. Then it checks its performance level with the state-of-the-art approaches. It depicts that, using the various performance measures; we can conclude that, our method achieves a greater value.

**Keywords:** Brain tumor MRI, image segmentation, image filtering, MR images, morphological filtering, image databases and performance metrics.

---

Date of Submission: 04-10-2021

Date of acceptance: 18-10-2021

---

## I. INTRODUCTION

Nowadays, brain tumor become a serious health issue, it may cause due to various circumstances such as chemical, radiation and genes. But not due to radiation from cell phone, person's fault, head injury etc. Some symptoms of brain tumor include headaches, persistent nausea and vomiting, loss of sensation, hearing loss, loss of vision, speech difficulties, confusion, memory loss etc. these are some of the early symptoms of brain tumor, so one can consult the expert's advice immediately and request on MRI should get the treatment sooner is better one. In the case of any doubtful tissues, doctor's may prefer MRI scan images than other type of scan images such as X-ray, CT etc. since it is free from any external disturbances such as usage of equipment, radiations etc. to identify the current situation of the patient. Through MR scan, experts can recognize the exact tumor region as well its. In order to pin point the exact location of the tumor region, segmentation technique is necessary[1].

Segmentation is done through various technology as it was thresholding, region- based, edge-based and clustering techniques etc. Contour based method [2,3, 4] can deal with noise, but the edge information is not preserved properly. Such poor segmentation is overcome in improved FCM clustering approach. The fourth order PDE reduces the noise found in an image and second order PDE detects the edge information [5]

Thresholding approach [6] works based totally on the histogram of the image, it doesn't need any earlier statistics of an image. However if huge amount of edge information is available, thresholding method does not segment out accurately, at the same time it is sensitive to dark areas. Also it does not provide an accurate segmented output under different lighting conditions. Edge detection technique [7] can effortlessly hit upon the edges with distinctive pixel intensities. Even though, it holds the edge content accurately, if any noise exists, the result was poor. It is overcome in region based segmentation [8]; however it consumes huge measure of time. Such time consumption is absolutely decreased in clustering algorithm [9], but there's a need of k value to acquire the clustered output. Recently FCM clustering is adapted, it is easy to implement but it does not provide fruitful result when it undergoes any variation of color on the surface of the object due to the presence of sunlight illumination, also if the image is subject to noise, it does not segment out the region properly. Also cluster's count used is unknown previously [10]. To overcome drawback of this, a possibilistic C- means technique is handed-down. It removes the noise thoroughly, but same clusters may occur repeatedly. This can be overcome by two improved possibilistic clustering method proposed, where it avoids the same clusters by modifying the objective function, an inversion function is included while calculating the distance between centers of two clusters. Another method to overcome the drawback of FCM[11] is that by altering the membership function which was proposed.

Even though the segmentation approaches are used to detect the tumor region exactly, but also it undergoes certain issues due to the noisy environment. Such noisy effect is reduced through image pre-processing technique. The abolishment of noise is considered as principal errand. In image pre-processing, it

undergoes various filtering techniques. Noise filter will smoothen out the noise content in the image and neutralize it with the original image content. The noise may be low frequency or high frequency, it is said to be removed by noise filtering technique.

Median filter preserves the edge details more accurately based on the mask size. If the mask size is smaller, the result will be very poor. At the same time, it may loss some significant details of the image. Histogram equalization method [12] improves the intensity of the image, but it won't works well with noise. For most medical image processing applications, wavelet transform is used for filtering, but it losses the edge smoothness. Dual tree wavelet transform is better than the wavelet transform, since it can separate out the texture details more accurately. Gaussian filter [13] uses low pass filter for the filtering operation, it removes all high frequency noise in the noise contaminated image. Also it keeps the edge as a sharper one. But it does not works well when it is encountered any illumination condition. Kalman filtering algorithm uses the procedure of recursive algorithm, where it works well, also it is computationally more efficient. But the major drawback is that, it is not suitable for any real time works.

The major work of the paper is

- i. Obtain the MR image from the BRATS database [14].
- ii. Initially, it undergoes morphological top-hat filtering operation as pre-processing, to reduce noise when compared to other techniques such as [15].
- iii. Then segmentation is done by our novel method, where it overcomes the drawback of over segmentation [10], and sensitive to noise.
- iv. Later to the segmentation, its accuracy calculation is to be done through various performance metrics. In addition to this, comparison exists with the past works.

The remaining part of the paper has five different sections as: In section II, it encounters the problem related to the previous works, in section III, a detailed statistical explanation of our proposed work and in section IV, the results and its explanation are given. Finally in the last section V this paper is concluded.

## II. PREPROCESSING

In this section, we focused about filtering procedure. Initially, get the MR input image from the BRTAS dataset. Then image processing is accomplished to upgrade the class of the image. The upgraded image contains only the edge contents.

In this paper, we have utilized morphological filtering operation [17] as a pre-processing step to remove brighter areas. Morphological filtering operation is done with basic morphological operation, which includes erosion, dilation, opening and closing. In order to accomplish these basic operations, there is a demand of structuring element. Structuring element can be of any size and shape with a particular origin. The middle element of the structuring element is considered as origin. The basic operators include erosion and dilation [18], which performs the primary operators. Also the secondary operators are derived from the primary operators such as opening and closing. The erosion operator scrapes away the borders of foreground pixels. As a result of this foreground region acquire lesser in size than before. Structuring element is usually rectangular in size. In some cases it may appear as circular, elliptical or cross shaped kernel. The structuring element contains the data as zeros and ones.

For Dilation, let the binary content of the image is represented as B and the structuring element be  $S_t$ . Move  $S_t$  over B pixel by pixel, such that by placing origin at each pixel location and perform an OR operation between origin element in  $S_t$  and elements in B.

- i. The pixels in  $S_t$  is ideally matched with B, then the particular element is replaced by '1'.
- ii. The pixels in  $S_t$  is somewhat matched with B, then the particular element is replaced by '1'.
- iii. The pixels in  $S_t$  is not matched with B, then the particular element is replaced by '0'.

Similarly for erosion, move  $S_t$  over B pixel by pixel, such that by placing origin at each pixel location and perform an AND operation between origin element in  $S_t$  and elements in B.

- i. The pixels in  $S_t$  is ideally matched with B, then the particular element is replaced by '1'.
- ii. The pixels in  $S_t$  is somewhat matched with B, then the particular element is replaced by '0'.
- iii. The pixels in  $S_t$  is not matched with B, then the particular element is replaced by '0'.

In opening, erosion is followed by dilation, at the same time both uses the same structuring element. It reduces the pixels which are grouped as smaller one in the foreground region. The equation for opening is stated as follows

$$B \circ S_t = (B \ominus S_t) \oplus S_t \tag{1}$$

Initially opening performs erosion, and then it performs dilation. Dilation rebuilds the structure of an object. So by means of an opening morphological operator, we can asset the object in which a distinct  $S_t$  is good enough. The Top hat filtering performs the subtraction operation between input image F and opened image. The top hat filtering operation, P is stated as

$$P = F - B \circ S_t \tag{2}$$

It holds the brightness area of an image.

### III. IMAGE SEGMENTATION

A novel procedure is initiated to obtain the tumor region from the pre-processed region. So, the resultant region contains the tumor region as brighter area, as well the background region, which was replaced as darker areas. The function ‘F’ characterize the segmented output using the equation as

$$F = 3 \times \exp\left(\frac{(p_{cd} + a + b)^3}{\sqrt{3}}\right) \tag{3}$$

Where  $p_{cd}$  point out clearly the pixel values in the filtered image  $c=1,2,3,\dots,r$ ,  $d=1,2,3,\dots,s$ .  $r$  be the row size and  $s$  be the column size of the image

The function ‘F’ rely on the parameters  $a$  and  $b$  and this can be given as

$$a = \frac{1}{\pi} \exp\left(- (m \times v)^2\right) \tag{4}$$

$$b = \frac{1}{\pi} (m + v) \tag{5}$$

Here  $m$  and  $v$  stipulates the mean and variance of the image.

Generally mean includes arithmetic mean, geometric mean, harmonic mean and contra harmonic mean. In our work we considered arithmetic mean [19]; it operates on  $c \times d$  window. By computing the average of all pixels presents in a window and replaces the central pixel by its average value. Likewise the process continues, till it reaches the last pixel value.

The mean value ‘ $m$ ’ is quantified as follows

$$m = \frac{1}{rs} \sum_{c=1}^r \sum_{d=1}^s p_{cd} \tag{6}$$

Where  $p_{cd}$  input image,  $c$  and  $d$  are the row and column size of an image.

Similarly the variance of an image is assessed as follows

$$v = \frac{1}{rs} \sum_{c=1}^r \sum_{d=1}^s (p_{cd} - m)^2 \tag{7}$$

By utilizing the mean and variance, we acquire the constant parameters such as  $a$  and  $b$ .

The algorithm of the segmentation approach is given as:

- i. The input image is assumed for segmentation as P (Filtered output).
- ii. Perform the segmentation process on the filtered image.
  - (a) Compute the mean ‘ $m$ ’ and variance ‘ $v$ ’ of the filtered image.
  - (b) Next, it compute the parameters  $a$  and  $b$ (using equation (4) and (5)), as it depends on ‘ $m$ ’ and ‘ $v$ ’
- iii. Determine the function ‘F’ using equation (3), which generates the segmented output.

Now the function ‘F’ is obtained. Then the segmented output is compared with ground truth images for comparison.

#### IV. PERFORMANCE EVALUATION

Based on segmentation accuracy, one can analyze that which method works well. So here in our work, we focused on the performance metrics such as PSNR, MSE, RMSE, SSIM and Dice.

PSNR:

It estimates the conflict among the maximum signal power and MSE [20]. PSNR is depicted as

$$PSNR = 10 \log \left( \frac{Max_{cd}^2}{MSE} \right) \quad (8)$$

MSE (Mean Square Error):

It calculates the average of the sum of the error occurs between the ground truth and the segmented output image [20, 21]. It can be calculated as

$$MSE = \frac{1}{rs} \sum_{c=0}^{r-1} \sum_{d=0}^{s-1} [g_{cd} - f_{cd}]^2 \quad (9)$$

Where  $g_{cd}$  represents pixel of the ground truth image of size  $c \times d$ . Similarly  $f_{cd}$  represents pixel of the segmented output image of size  $c \times d$ .

RMSE (Root Mean Square Error):

The massive value of RMSE indicates significant variation between the ground truth and the reproduced image [20, 21].

$$RMSE = \sqrt{\frac{1}{rs} \sum_{c=0}^{r-1} \sum_{d=0}^{s-1} [g_{cd} - f_{cd}]^2} \quad (10)$$

Dice:

The relationship involving ground truth 'G' and segmented image 'F' such that, it computes the ratio of the common to the sum of number of elements between them.

$$Dice = \frac{2|G \cap F|}{|G| + |F|} \quad (11)$$

SSIM (Structural Similarity Index Measure):

It relies on the function of luminance, contrast and structure of the two images (ground truth, G and segmented image F).

$$SSIM(G, F) = g(Lu(G, F), Co(G, F), St(G, F)) \quad (12)$$

$Lu(G, F)$ ,  $Co(G, F)$  and  $St(G, F)$  be the luminance, contrast and the structural comparison between the images G and F, it is given as

$$Lu(G, F) = \frac{2m_G m_F + K_1}{m_G^2 + m_F^2 + K_1} \quad (13)$$

$$Co(G, F) = \frac{2S_G S_F + K_2}{S_G^2 + S_F^2 + K_2} \quad (14)$$

$$St(G, F) = \frac{S_{GF} + K_3}{S_G S_F + K_3} \quad (15)$$

$m_G$  and  $m_F$  reveals the mean value G and F.  $S_G$  and  $S_F$  stipulates the standard deviation of G and F.

$K_1, K_2$  and  $K_3$  are small positive value constants.

#### V. EXPERIMENTAL RESULTS

In this section, it clearly explains how our implementation is carried out throughout to improve the accuracy by simulation results. The input images of our proposed work are obtained from the BRATS dataset [14] shown in figure1. The abnormal image is considered in my work of size 256x 256. Three different steps convey our work. First, it performs morphological filtering operation for the input image. The

filtered image undergoes novel segmentation was included in the second set. Thirdly, it employs the detailed evaluation of segmentation accuracy. It depicts that our proposed work gain better value in terms of performance measure.

### 5.1. Morphological filtering operation

The pre-processing is experienced with morphological filtering, in order to remove the noise available in an image. It occurs due to the equipment used during scanning. So it should be removed previously to segmentation to produce an accurate output [22]. The morphologically filtering operation is done through top-hat filtering, where it reduces the noise in an image is represented in figure. 2. From the figure, we can conclude that the tumor region is highly enhanced, when compared to the background region.

### 5.2. Segmentation based on novel method

The filtered output holds the tissue information brighter than other areas. Then, that brighter area or the tissue region is separate it out by segmentation. Segmentation operation is performed to point out the exact region of the tumor area [23]. By using  $m$  and  $v$ , the parameters  $a$  and  $b$  is computed using equation (4) and (5). Afterwards, the function  $F$  is deliberated using equation (3). Conclusively we acquire the segmented output is as shown in figure. 3.

It depicts that brighter area from the filtered output is segmented properly. The exact detail about the segmented image is extracted based on the segmentation accuracy. The accuracy calculation is quantified between the ground truth and segmented images through various performance measures. The ground truth images are used in performance calculation, since expert's need to confirm whether the segmented out is correct or not. So as to bring correct notification, ground truth images are used. It is shown in figure. 4. For an accuracy calculation, the comparison exists between different techniques with various performance comparison measures. Figure 5 exhibits the numerous approaches of segmentation such as FCM (Fuzzy C Means) in first row, Otsu method shown in second row and MRF (Markov Random Field) in third row. Now the segmentation accuracy is computed by various performance parameters such as PSNR, SSIM, Dice, RMSE and MSE, between segmented output of novel approach and ground truth image as well as the comparison is made with the previous works.

In this study, we proposed a novel method based on distribution function for an automatic obtainment of segmented output from the filtered images. But it becomes a performance was by comparing the similarity between the segmented output and the expert's analysed output with challenging issue to evaluate the performance of automatic computation method to obtain the segmented output using MR images. The evaluation method used to compute the PSNR, MSE, RMSE, SSIM and Dice. The expert's analyzed tumor region as ground truth images, also in some cases manual segmentation is performed, while comparing the manual segmented output with expert's analyzed output, the results obtained from manual segmentation yields poor quality results. Furthermore, in computation with the state- of- the- art methods, the proposed method outperformed in all the performance metrics. This is due to the attribution of the novel distribution function. The entire process is done automatically without any manual involvement. Thus it saves time and avoids manual assignment of variables or parameters.

While comparing with the proposed method, FCM, algorithm needs manual assignment of variable. The Otsu's algorithm works based on threshold value obtained from the histogram of the image. But the output is poor, when the input image is subject to various illumination conditions. The MRF method is considered as an inefficient one in computation. Our proposed algorithm overcomes the above said existing problems on BRATS datasets, as an automatic implementation algorithm for the computation of tumor region.

Here, we have explored the algorithm using MATLAB programming for implementation to assess the tumor region exactly.

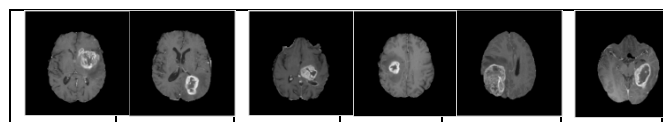


**Figure1: Input images from BRATS dataset**

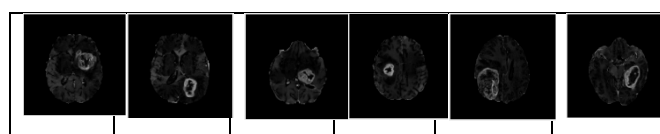


**Figure2: Top-hat filtered output**

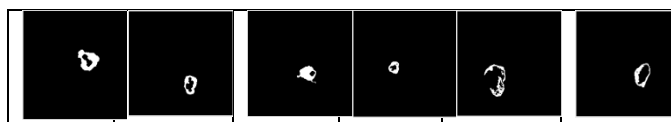


Figure 3; Novel segmented output

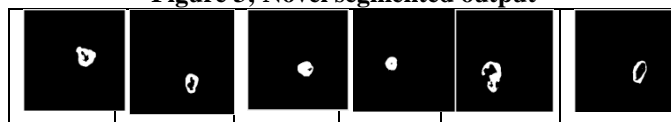


Figure4: Ground truth images.

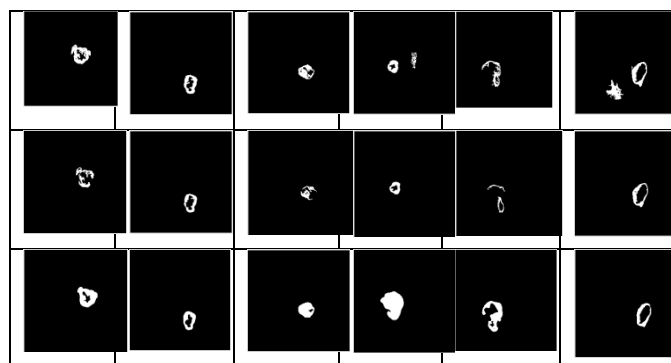


Figure5: Segmented results of various methods, FCM in the first row, Otsu method in the second row and MRF method in the third row.

Table 1: Performance measures

Images	PSNR				Dice			
	Otsu	FCM	MRF	Proposed	Otsu	FCM	MRF	Proposed
Image1	16.3309	22.2476	15.0116	<b>23.1052</b>	0.0036	0.1472	0.0045	<b>0.1520</b>
Image2	18.8938	26.0247	16.4153	<b>26.4656</b>	0.0052	0.2295	0.0030	<b>0.2459</b>
Image3	17.6450	23.4059	16.7586	<b>24.0590</b>	0.0026	0.2086	0.0052	<b>0.1965</b>
Image4	19.3006	21.3647	17.3322	<b>22.9254</b>	0.0036	0.2426	0.0123	<b>0.2993</b>
Image5	15.6101	17.5438	14.7175	<b>17.5737</b>	0.0014	0.1611	0.0053	<b>0.1526</b>
Image6	19.2505	17.4058	17.5833	<b>22.7670</b>	0.0060	0.1639	0.0040	<b>0.2337</b>
Average	17.8384	21.3321	16.3031	<b>22.8160</b>	0.0037	0.1922	0.0057	<b>0.2133</b>

Images	RMSE				SSIM			
	Otsu	FCM	MRF	Proposed	Otsu	FCM	MRF	Proposed
Image1	38.9039	19.6861	45.2856	<b>17.8354</b>	0.0001	0.9653	0.9087	<b>0.9681</b>
Image2	28.9633	12.7440	38.5277	<b>12.1132</b>	0.0001	0.9842	0.9154	<b>0.9853</b>
Image3	33.4418	17.2284	37.0350	<b>15.9805</b>	0.0001	0.9730	0.9405	<b>0.9767</b>
Image4	27.6383	21.7924	34.6683	<b>18.2083</b>	0.0001	0.9641	0.9353	<b>0.9774</b>
Image5	42.2702	33.8336	46.8454	<b>33.7175</b>	0.0001	0.9422	0.9083	<b>0.9423</b>
Image6	27.7982	34.3755	33.6802	<b>18.5435</b>	0.0001	0.9391	0.9448	<b>0.9726</b>
Average	33.1693	23.2767	39.3404	<b>19.3997</b>	0.0001	0.9613	0.9255	<b>0.9704</b>

Images	MSE			
	Otsu	FCM	MRF	Proposed
Image1	1513.5000	387.5440	2050.8000	<b>318.0997</b>
Image2	838.8714	162.4101	1484.4000	<b>146.7291</b>

Image3	1118.4000	296.8184	1371.6000	<b>255.3758</b>
Image4	763.8748	474.9094	1201.9000	<b>331.5406</b>
Image5	1786.8000	1144.7000	2194.5000	<b>1136.9000</b>
Image6	772.7423	1181.7000	1134.4000	<b>343.8613</b>
Average	1132.3648	608.0165	1572.9333	<b>422.0844</b>

### 5.3. Segmentation accuracy

For these segmented images, its accuracy is computed by various performance parameters such as PSNR, MSE, RMSE, SSIM and Dice is given in the following tables. It depicts that the highest value is obtained for PSNR, SSIM and Dice and lowest value is for RMSE and MSE.

Table 1 demonstrates that the PSNR, Dice, RMSE, SSIM and MSE attains as an average value of 22.8160, 0.2133, 0.9704, 19.3997 and 422.0844 respectively. The PSNR value is higher when compared to Otsu, FCM and MRF model in the range of 21.82%, 6.5% and 28.55% respectively. Similarly, the Dice coefficient is improved by 98.27%, 9.89% and 97.33% than Otsu, FCM and MRF techniques. Finally SSIM is increased by 99.98%, 0.94% and 4.63% than Otsu, FCM and MRF respectively. Also, MSE and RMSE is less when compared to the previous methods.

## VI. CONCLUSION

The abnormal growth in the brain region is pointed out properly by a novel segmentation approach. Initially morphological top-hat filtering is performed to promote the edge information of the image. At that point, it experiences segmentation by the novel strategy to extricate the tumor area. Simulation result depicts that the average estimation of the proposed methodology gives better accuracy for the five performance measurements with the ground truth images. The evaluation estimates determined on segmentation yield that, it accomplishes higher as an average of 22.8160, 0.2133 and 0.9704 for PSNR, Dice and SSIM and lower as an average of 19.3997 and 422.0844 for RMSE and MSE respectively. The segmentation result portrays that the proposed calculation improves the nature of tumor region. The investigation has revealed that the output is nearer to the ground truth images accessible in BRATS database.

## REFERENCES

- [1]. Brain Tumor and Brain Cancer, Retrieved from: <http://www.cedars-sinai.edu/Patients/Health-Conditions/Brain-Tumors-and-Brain-Cancer.aspx>, Retrieved on: 3 Dec (2013).
- [2]. N. T. N. Anh, J. Cai, J. Zhang, and J. Zheng, (2012) , "Constrained active contours for boundary refinement in interactive image segmentation," in IEEE International Symposium on Circuits and Systems (ISCAS), pp. 870-873.
- [3]. M. A. Savelonas, E. A. Mylona, and D. Maroulis, (2012), "Unsupervised 2D gel electrophoresis image segmentation based on active contours," Pattern Recognition, vol. 45, pp. 720-731.
- [4]. B. Wu and Y. Yang, (2012), "Local-and global-statistics-based active contour model for image segmentation," Mathematical Problems in Engineering, vol. 2012.
- [5]. M. Yambal and H. Gupta, (2013) "Image Segmentation using Fuzzy C Means Clustering: A survey", International Journal of Advanced Research in Computer and Communication Engineering, Vol. 2, Issue 7.
- [6]. K.K. Singh, A. Singh, (2010) "A Study of Image Segmentation Algorithms for Different Types of Image", International Journal of Computer Science Issues, Vol. 7, Issue 5.
- [7]. H.P.Narkhede, (2010), "Review of Image Segmentation Techniques", ISSN: 2319 - 6386, vol.1, Issue-8, (2013).
- [8]. J. Tang, "A Color Image Segmentation algorithm Based on Region Growing," in Proc. IEEE Trans. Electrical Engineering, Conf., pp. 634-637.
- [9]. S. Naz, H. Majeed, H. Irshad, (2010), "Image Segmentation using Fuzzy Clustering: A Survey", International Conference on ICET, pp. 181-186.
- [10]. J.C. Bezdek., "Pattern recognition with fuzzy objective function algorithm," (Pentium press, New York).
- [11]. Pham. D. L, (2002), "Fuzzy clustering with spatial constraints," IEEE proceedings of international conference on image processing, pp. 65-68.
- [12]. P. Babu, V. Rajamani, (2015), "Contrast enhancement using real coded genetic algorithm based modified histogram equalization for gray scale images," Int. Journal of imaging system technol., vol. 25, no. 1, pp. 24-32.
- [13]. <https://en.wikipedia.org/wiki/Gaussain-filter>.
- [14]. <https://www.smir.ch/BRATS/Start2015>.
- [15]. T. Kao, Len-Jon Hwang, Yui-Han Lin, Tzong-Huei Lin and Chia-Hung Hsiao, (2001),"Computer Analysis of the Electrocardiograms from ECG Paper recordings", Proceedings of the23rd AnnualEMBSInternationalConference,Istanbul,Turkey,pp.3232-3234.
- [16]. Fei Wang Tanveer Syeda-Mahmood David Beymer, (2009)"Information Extraction from Multimodal ECG Documents," 10th International Conference on Document Analysis and Recognition.
- [17]. R.C. Gonzalez, Richard E. Woods, (1992) "Digital image processing", Wiley.
- [18]. P. Soille, (2003) "Morphological Image Analysis: Principles and Applications", Engineering Online Library. Springer, Berlin, Germany, 2nd edition.

- [19]. Vijay Kumar, Priyanka Gupta, (2012), "Importance of statistical measures in digital image processing", International journal of emerging technology and advanced engineering, volume 2, issue 8, pp.56-62.
- [20]. Amritpal Kaur, Amandeep Kaur, (2014), "Evaluation of parameters of image segmentation algorithms-JSEG and ANN", International journal of advanced research in electronics and communication engineering (IJARECE), Vol. 3, Issue. 8, pp. 854-865.
- [21]. D. Manju, M. Sheetha, K. Venugopala Rao, (2013), "Comparative study of segmentation technique for brain tumor detection" international journal of computer science and Mobile computing, vol. 2, Issue. 11, pp. 261-269.
- [22]. R. Remya, K. Parimala Geetha, S. Sundaravadevelu, (2019), "Enhanced DWT filtering technique for brain tumor detection", international Journal of Research, <https://doi.org/10.1080/03772063.2019.1656555>.
- [23]. Remya. R, Parimala Geetha. K & Murugan. S (2020), "A series of exponential function, as a novel methodology in detecting brain tumor", Biomedical Signal Processing and Control, Elsevier, vol. 62, pp. 1-21.